Using Amide ^{1}H and ^{15}N Transverse Relaxation To Detect Millisecond Time-Scale Motions in Perdeuterated Proteins: Application to HIV-1 Protease

Rieko Ishima,[†] Paul T. Wingfield,[‡] Stephen J. Stahl,[‡] Joshua D. Kaufman,[‡] and Dennis A. Torchia*,[†]

Contribution from the Molecular Structural Biology Unit, National Institute of Dental Research, and Protein Expression Laboratory, National Institute of Arthritis and Musculoskeletal and Skin Diseases, National Institutes of Health, Bethesda, Maryland 20892

Received May 4, 1998. Revised Manuscript Received August 10, 1998

Abstract: Measurements of proton transverse relaxation rates, R_2 and $R_{1\rho}$, have not been commonly performed for proteins because cross correlations among the numerous ^{1}H−^{1}H dipolar interactions complicate analysis of the data. In addition, these interactions make large contributions to the relaxation of the amide protons, making it difficult to detect if an exchange of chemical shifts also makes a contribution, R_{ex}, to relaxation. To overcome these problems, we have investigated proton relaxation of a perdeuterated protein, HIV-1 protease, bound to a small protonated inhibitor DMP323. Perdeuteration significantly reduces the contributions of ^{1}H−^{1}H dipolar interactions to the relaxation of the amide protons. The ROESY $R_{1\rho}$ experiment further reduces the overall relaxation rate as compared with the usual $R_{1\rho}$ experiment because the protons relax as unlike spins, with rate $R_{1\rho,\text{unlike}}$, in the former experiment but as like spins, with rate $R_{1\rho}$, in the latter. These reductions of the proton transverse-relaxation rate facilitated the detection of R_{ex} contributions at several sites in the protein (1) from the B_1-field dependence of $R_{1\rho,\text{unlike}}$ and (2) by comparing $R_{1\rho,\text{unlike}}$ values with relaxation rates, R_2, obtained from Carr−Purcell−Meiboom−Gill (CPMG) and Hahn-echo experiments. The significant reduction of the proton spin-flip rate in the perdeuterated protein enabled measurement of ^{15}N R_2 values using the CPMG method and the same large duration between 180° pulses as used in the ^{1}H CPMG experiments. Hence, relaxation data of both nuclei were utilized to obtain complementary information about sites experiencing exchange of chemical shifts in the protein.

Introduction

Recent advances in indirect proton detection of heteronuclear magnetization[1−3] together with isotopic enrichment techniques have enabled ^{15}N and ^{13}C spin relaxation to become widely used to relate molecular flexibility and biological function of proteins.[4−12] For this purpose, a variety of approaches has been applied because proteins undergo internal motions on a wide range of time scales. Longitudinal and transverse relaxation, together with the NOE, have been commonly used to detect internal motions faster than the rotational correlation time of the protein. In addition, indirect detection techniques that provide relaxation times of ^{2}H spins have been developed that are particularly useful for characterizing motions of methyl groups in proteins.[13] To detect slow conformational fluctuations (that modulate isotropic chemical shifts) on the millisecond to microsecond time scale, relaxation rates have been measured using either a Carr−Purcell−Meiboom−Gill (CPMG) sequence or a spin lock.[14,15] Recently off-resonance rotating-frame relaxation measurements have successfully yielded the rates of such conformational fluctuations of individual sites in proteins.[16−18]

Unlike natural abundance ^{2}H, ^{13}C, and ^{15}N spins, which are rare in proteins and have small magnetogyric ratios, protons are ubiquitous and have large magnetic moments. Hence, each proton typically experiences numerous dipolar interactions with neighboring protons, and ^{1}H spin-diffusion rather than molecular motion determines its longitudinal relaxation.[19] Furthermore, the

† National Institute of Dental Research.
‡ National Institute of Arthritis and Musculoskeletal and Skin Diseases.
* Corresponding author. E-mail: torchia@yoda.nidr.nih.gov. Phone: 301-496-5750. Fax: 301-402-1512.

(1) Mueller, L. *J. Am. Chem. Soc.* **1979**, *101*, 4481−4484.
(2) Morris, G. A.; Freeman, R. *J. Am. Chem. Soc.* **1979**, *101*, 760−762.
(3) Bodenhausen, G.; Ruben, D. J. *Chem. Phys. Lett.* **1980**, *69*, 185−189.
(4) Nirmala, N. R.; Wagner, G. *J. Am. Chem. Soc.* **1988**, *110*, 7557−7558.
(5) Kay, L. E.; Torchia, D. A.; Bax, A. *Biochemistry* **1989**, *28*, 8972−8979.
(6) Schneider, D. M.; Dellwo, M. J.; Wand, A. J. *Biochemistry* **1989**, *31*, 3645−3652.
(7) Clore, G. M.; Driscoll, P. C.; Wingfield, P. T.; Gronenborn, A. M. *Biochemistry* **1990**, *29*, 7387−7401.
(8) Palmer, A. G. *Curr. Opin. Biotechnol.* **1993**, *4*, 385−391.
(9) Fushman, D.; Ohlenschlager, O.; Ruterjans, H. *J. Biomol. Struct. Dyn.* **1994**, *11*, 1377−1402.
(10) Peng, J. W.; Wagner, G. *Biochemistry* **1995**, *34*, 16733−16752.
(11) Yamasaki, K.; Saito, M.; Oobatake, M.; Kanaya, S. *Biochemistry* **1995**, *34*, 6587−6601.
(12) Dayie, K. T.; Wagne, G.; Lefevre, J. F. *Annu. Rev. Phys. Chem.* **1996**, *47*, 243−282.
(13) Muhandiram, D. R.; Yamazaki, T.; Sykes, B. D.; Kay, L. E. *J. Am. Chem. Soc.* **1995**, *117*, 11536−11544.
(14) Abragam, A. *Principles of Nuclear Magnetism*; Oxford University Press: Oxford, U.K., 1961.
(15) Luz, Z.; Meiboom, S. *J. Chem. Phys.* **1963**, *39*, 366−370.
(16) Berthault, P.; Birlirakis, N.; Rubinstenn, G.; Sinay, P.; Desvaux, H. *J. Biomol. NMR* **1996**, *8*, 23−35.
(17) Akke, M.; Palmer, A. G. *J. Am. Chem. Soc.* **1996**, *118*, 911−912.
(18) Akke, M.; Liu, J.; Cavanagh, J.; Erickson, H.; Palmer, A. G. *Nat. Struct. Biol.* **1998**, *5*, 55−59.

S0002-7863(98)01546-7 CCC: $15.00
Published on Web 09/24/1998

proton transverse relaxation rate is difficult to interpret because of dipolar cross correlation among the numerous $^1H-^1H$ dipolar interactions.[20] These interactions also strongly depend on the interproton distances that vary if the molecule is flexible. Finally, it is often difficult to detect R_{ex} (the relaxation rate resulting from exchange of the isotropic chemical shift) contributions to relaxation, in the presence of these large dipolar interactions. For these reasons the proton has seldom been used to probe dynamics of large proteins, despite the potential advantage that a larger range of the spin-locking field, γB_1 (in hertz), can be used for the proton because of its large magnetogyric ratio.[21] Hence, quantitative analysis of ^1H relaxation has been limited to small molecules.[22−25]

One method to reduce, if not completely eliminate, the problems associated with strong $^1H-^1H$ dipolar interactions is to use a protein in which the nonlabile protons are replaced with deuterium.[26−28] This approach restricts the major dipolar interactions of an ^1H amide to those with its neighboring amide ^1H spins and its directly bonded ^{15}N spin and thereby increases the relative contribution from exchange, R_{ex}, to the total transverse relaxation rate. We extended this strategy of maximizing the R_{ex} contribution to the total relaxation rate in two ways. We developed a ROESY (rotating frame Overhauser enhancement spectroscopy) $R_{1\rho}$ (relaxation rate in the rotating frame) experiment and used it in place of the normal ^1H $R_{1\rho}$ experiment to measure the ^1H rotating frame relaxation rate. In the ROESY-type $R_{1\rho}$ experiment the protons relax as unlike spins,[29] with rate $R_{1\rho,\text{unlike}}$ (unlike-spin relaxation rate in the rotating frame), significantly reducing the $^1H-^1H$ dipolar contribution to the relaxation rate. We also used the cross correlation of the ^1H chemical shift anisotropy and the $^1H-^{15}N$ dipolar interaction to reduce the amide proton relaxation rate by measuring the relaxation rate of upfield component of the proton $^1J_{HN}$ doublet.[30]

^{15}N relaxation experiments benefit from perdeuteration as well. In the case of protonated proteins, rapid ^1H spin-flips cause $^{15}N_{x,y}H_z$ antiphase magnetization to relax significantly faster than $^{15}N_{x,y}$ inphase magnetization. The ^1H spin-flips also act to average the relaxation rates of the two $^1J_{HN}$-coupled components. Consequently, as the duration between 180° pulses in the CPMG sequence increases so does the apparent ^{15}N transverse relaxation rate. For this reason, CPMG experiments are typically recorded using $\tau_{CPMG} < 0.75$ ms, where $2\tau_{CPMG}$ is the period between ^{15}N 180° pulses. However, deuterating the protein isolates the amide protons and ^1H spin-flips contribute much less to the $^{15}N_{x,y}H_z$ relaxation. Hence, ^{15}N R_2 (transverse relaxation rate) values can be accurately measured using τ_{CPMG} values of several milliseconds, as we show below.

Herein, we first report the $R_{1\rho}$ and $R_{1\rho,\text{unlike}}$ values of the amide protons of ^{15}N-enriched perdeuterated HIV-1 (human immunodeficiency virus-1) protease, bound to the inhibitor DMP323 ($K_D = 0.25$ nM[47]). $R_{1\rho,\text{unlike}}$ of the amide protons are compared with R_2 values measured by CPMG and Hahn-echo experiments and with $R_{1\rho,\text{unlike}}$ values calculated using $^1H-^1H$ distances derived from X-ray coordinates. Next, we report amide ^{15}N $R_{1\rho}$ and CPMG R_2 measurements of perdeuterated HIV-1 protease. Our primary goals are to (1) identify each amino acid residue whose amide proton relaxation contains an R_{ex} contribution, from measurements of the B_1 field dependence of $R_{1\rho,\text{unlike}}$ and from the comparison of $R_{1\rho,\text{unlike}}$ with R_2, and (2) better characterize the conformational fluctuations that are the source of the R_{ex} contribution, from measurement of both ^1H and ^{15}N transverse relaxation.

Previous studies of the structure and dynamics of the protease have demonstrated flexibility of the flaps (each consisting of a two-stranded β-sheet connected by a β-turn, residues 49−52) which extend over the substrate binding cleft[31−37] and are important for protease activity.[38] ^{15}N NMR relaxation experiments performed at 35 °C demonstrated conformational exchange of the β-turn on the millisecond to microsecond time scale.[39] In addition, flexibility of the N-terminal loop (the primary autolysis site in the protein) on millisecond to microsecond time scale was inferred from a model-free[40] analysis of the reduced ^{15}N transverse relaxation times of neighboring residues 3, 8, and 98.[39]

Methods and Materials

Proton relaxation rates in the rotating frame were measured using the pulse sequences shown in Figure 1. Like ^{15}N relaxation experiments these sequences (1) maximize sensitivity by using proton spins for source and detected magnetization and (2) increase resolution by recording evolution in two (^{15}N and ^1H) dimensions. Sequences designed to measure (A) $R_{1\rho}$ and (B) $R_{1\rho,\text{unlike}}$ differ from one another in that the proton relaxation period precedes the ^{15}N evolution period in A, while the reverse is true in B. Hence in A the full steady-state magnetization of every amide proton is locked along the same axis and the proton−proton dipolar relaxation rate is that of

(19) Kalk, A.; Berendsen, H. J. C. *J. Magn. Reson.* **1976**, *24*, 343−366.
(20) Werbelow, L. G.; Grant, D. M. In *Advances in Magnetic Resonance*; Waugh, J. A., Ed.; Academic Press: New York, 1997; Vol. 9, pp 190−299.
(21) Almeida, F. C.; Opella, S. J. *J. Magn. Reson.* **1997**, *124*, 509−511.
(22) Niccolai, N.; Pogliani, L.; Rossi, C.; Corti, P.; Gibbons, W. A. *Biophys. Chem.* **1983**, *20*, 217−223.
(23) Marion, D.; Genest, M.; Ptak, M. *Biophys. Chem.* **1987**, *28*, 235−244.
(24) Borgias, B. A.; James, T. L. *Methods. Enzymol.* **1989**, *176*, 169−183.
(25) Blackledge, M. J.; Bruschweiler, R.; Griesinger, C.; Schmidt, J. M.; Xu, P.; Ernst, R. R. *Biochemistry* **1993**, *32*, 10960−10974.
(26) Matthews, K. S.; Wade-Jardetzky, N. G.; Graber, M.; Conover, W. W.; Jardetzky, O. *Biochim. Biophys. Acta* **1977**, *490*, 534−538.
(27) LeMaster, D. M. *FEBS Lett.* **1987**, *223*, 191−196.
(28) Torchia, D. A.; Sparks, S. W.; Bax, A. *J. Am. Chem. Soc.* **1988**, *110*, 2320−2321.
(29) (a) Bothner-By, A. A.; Stephens, R. L.; Lee, J.-m.; Warren, C. D.; Jeanloz, R. W. *J. Am. Chem. Soc.* **1984**, *106*, 811−813. (b) Cavanagh, J.; Fairbrother, W. J.; Palmer, A. G.; Skelton, N. J. *Protein NMR Spectroscopy*; Academic Press Inc.: San Diego, CA, 1996; Chapter 5.
(30) Pervushin, K.; Riek, R.; Wider, G.; Wutrich, K. *Proc. Natl. Acad. Sci. U.S.A.* **1997**, *94*, 12366−12371.
(31) Lapatto, R.; Blundell, T.; Hemmings, A.; Overington, J.; Wilderspin, A.; Wood, S.; Merson, J. R.; Whittle, P. J.; Danley, D. E.; Geoghegan, K. F.; Hawrylik, S. J.; Lee, S. E.; Scheld, K. G.; Hobart, P. M. *Nature* **1989**, *342*, 299−302.
(32) Navia, M. A.; Fitzgerald, P. M.; McKeever, B. M.; Leu, C. T.; Heimbach, J. C.; Herber, W. K.; Sigal, I. S.; Darke, P. L.; Springer, J. P. *Nature* **1989**, *337*, 615−620.
(33) Wlodawer, A.; Miller, M.; Jaskolski, M.; Sathyanarayana, B. K.; Baldwin, E.; Weber, I. T.; Selk, L. M.; Clawson, L.; Schneider, J.; Kent, S. B. *Science* **1989**, *245*, 616−621.
(34) Harte, W. E. J.; Swaminathan, S.; Mansuri, M. M.; Martin, J. C.; Rosenberg, I. E.; Beveridge, D. L. *Proc. Natl. Acad. Sci. U.S.A.* **1990**, *87*, 8864−8868.
(35) York, D. M.; Darden, T. A.; Pedersen, L. G.; Anderson, M. W. *Biochemistry* **1993**, *32*, 1443−1453.
(36) Yamazaki, T.; Hinck, A. P.; Wang, Y. X.; Nicholson, L. K.; Torchia, D. A.; Wingfield, P.; Stahl, S. J.; Kaufman, J. D.; Chang, C. H.; Domaille, P. J.; Lam, P. Y. *Protein Sci.* **1996**, *5*, 495−506.
(37) Ala, P. J.; Huston, E. E.; Klabe, R. M.; McCabe, D. D.; Duke, J. L.; Rizzo, C. J.; Korant, B. D.; DeLoskey, R. J.; Lam, P. Y.; Hodge, C. N.; Chang, C. H. *Biochemistry* **1997**, *36*, 1573−1580.
(38) Shao, W.; Everitt, L.; Manchester, M.; Loeb, D. D.; Hutchison, C. A. R.; Swanstrom, R. *Proc. Natl. Acad. Sci. U.S.A.* **1997**, *94*, 2243−2248.
(39) Nicholson, L. K.; Yamazaki, T.; Torchia, D. A.; Grzesiek, S.; Bax, A.; Stahl, S. J.; Kaufman, J. D.; Wingfield, P. T.; Lam, P. Y.; Jadhav, P. K. *Nat. Struct. Biol.* **1995**, *2*, 274−280.
(40) Lipari, G.; Szabo, A. *J. Am. Chem. Soc.* **1982**, *104*, 4546−4559.

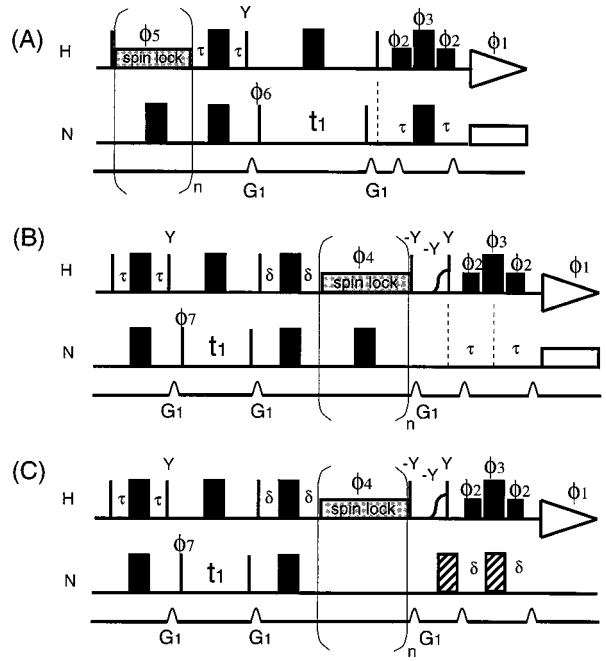

Figure 1. Pulse sequences used to measure transverse proton relaxation rates of inhibited HIV-1 protease. Sequences used to measure (A) $R_{1\rho}$, (B) $R_{1\rho,\text{unlike}}$, and (C) $R_{1\rho,\text{unlike}}$. Narrow and wide pulses correspond to flip angles of 90° and 180° pulses, respectively, and are along X unless noted otherwise. The two low power pulses immediately preceding and following the last nonselective ^{1}H 180° pulse had widths of 1 ms each and correspond to flip angles of 90°. A half-Gauss 90° pulse of 2 ms was used prior to the final 90° hard pulse, and delays δ and τ were 2.7 and 2.2 ms, respectively. The phase cycle was $\phi_1 = X, -X$; $\phi_2 = -X, X$; $\phi_3 = X, X, -X, -X$; $\phi_4 = 4X, 4(-X)$; $\phi_5 = 4(Y), 4(-Y)$; $\phi_6 = Y, -Y$; $\phi_7 = X, -X$. Quadrature detection in the t_1 dimension was achieved by States-TPPI of ϕ_6 or ϕ_7. The proton on-resonance position was set to 4.7 ppm, except while spin locking, when it was shifted to 8.3 ppm. The strength of gradient was 25 G/cm, and its duration was either 1.5 ms for G_1 or 0.4 ms otherwise. In part C, the IPAP sequence[42] was used to measure the relaxation rates of the individual upfield and downfield components of the proton $^1J_{\text{HN}}$ doublet, with two interleaved data sets acquired either with or without the hatched 180° pulses.

like spins, $\lambda + \mu$, where λ and μ are the autorelaxation and cross relaxation rates, respectively.[41] In contrast, in B, evolution of the ^{15}N spins precedes the ^{1}H spin lock and the dipolar coupled protons relax as diagonal peaks in a ROESY experiment,[29] with relaxation rate $= \lambda$ (i.e., as unlike spins). When $(\mu t)^2/2 \ll 1$, where t is the spin-lock duration, and the attached ^{15}N spins have distinct chemical shifts, ROESY cross-peaks are a minor effect in a perdeuterated protein as we show later. Sequence B makes it easier to detect relaxation due to conformational exchange because it reduces the contribution of ^{1}H$-^1$H dipolar interactions to $R_{1\rho}$.

A further reduction of the proton relaxation rate is realized using the pulse sequence described in Figure 1C which uses an IPAP (in-phase antiphase) scheme similar to that described by Ottiger et al.[42] Two data sets, measured either with or without the hatched 180° pulses, are acquired in an interleaved manner using the scheme C, and the sum and difference of the data sets provide two spectra in which only either the downfield or upfield proton J multiplet component is observed. A reduction of the relaxation rate of the upfield $^1J_{\text{HN}}$ doublet component occurs because of partial cancellation of the ^{1}H$-^{15}$N dipolar and proton chemical shift anisotropy (CSA) interactions.[30] Note that the first hatched 180° pulse inverts the local dipolar field to compensate for the inversion by the second hatched 180° pulse.

In addition to measuring transverse magnetization in a spin-locked field, we also measured transverse relaxation, R_2, by replacing the spin-lock pulse in the $R_{1\rho,\text{unlike}}$ sequence in Figure 1B with either a CPMG or a Hahn-echo sequence. As is the case in the $R_{1\rho,\text{unlike}}$ experiment, the proton dipolar relaxation rate equals λ in the CPMG and Hahn-echo experiments. To compare proton relaxation rates with ^{15}N relaxation rates, ^{15}N $R_{1\rho}$ and CPMG R_2 experiments were performed at 20 °C using the sequences described previously.[39,43]

The ^{15}N-enriched perdeuterated protease−DMP323 complex was prepared as described.[44] Note that DMP323 was not deuterated. The NMR sample (250 μL in a Shigemi microcell) contained 0.35 mM protease dimer in $H_2O/^2H_2O$ (90%/10%), 20 mM sodium acetate buffer (pH 5.2), and 5 mM dithiothreitol. NMR spectra were acquired on Bruker DMX-500 spectrometer at temperatures 20 and 35 °C. Proton relaxation experiments were performed using six relaxation delays: 12, 24, 36, 48, 60, and 72 ms for CPMG and Hahn-echo R_2 and 6, 12, 18, 24, 30, and 36 ms for $R_{1\rho,\text{unlike}}$ and $R_{1\rho}$. The ^{1}H spin-locking field strength ranged from 2 to 6 kHz and from 2 to 12 kHz for the $R_{1\rho}$ and $R_{1\rho,\text{unlike}}$ experiments, respectively. In the CPMG pulse train, $(-\tau_{\text{CPMG}}-180°-\tau_{\text{CPMG}}-)_n$, τ_{CPMG} of 3 ms was used. Spectral widths of 1111.4 and 6009.6 Hz were set for F_1 and F_2 dimensions, respectively. ^{15}N $R_{1\rho}$ and CPMG R_2 rates[45] were measured at 20 °C using seven relaxation delays: 12, 24, 36, 48, 60, 72, and 84 ms. The ^{15}N spin-locking field strength was set to 2 kHz in the $R_{1\rho}$ experiment, while a τ_{CPMG} of 3 ms was used in the CPMG R_2 experiment. The total data collection time required to measure a single relaxation rate was ca. 20 h, using a recycle delay of ca. 3 s, 100 t_1, and 512 t_2 complex points. Data were processed using the nmrPipe software package,[46] and peak heights measured in the processed spectra were fitted with a two-parameter exponential function to extract relaxation rates. Errors of the relaxation rates were typically less than 5%. In the interest of clarity, error bars were not usually drawn in the figures, but residues for which errors are greater than 5% are noted in the figure captions. Off-resonance effects on ^{1}H $R_{1\rho,\text{unlike}}$ and ^{15}N $R_{1\rho}$ measurements were corrected using measured ^{1}H and ^{15}N longitudinal relaxation rates, R_1. To minimize off-resonance effects during CPMG experiments, hard 90° pulses were set as short as possible, i.e., 7.5 and 43.0 μs for ^{1}H and ^{15}N, respectively. Under these conditions, the errors in relaxation rates caused by the off-resonance effects in the CPMG experiments were estimated to be less than 2%.[47]

For purposes of comparing experiment and theory, $R_{1\rho,\text{unlike}}$ values of the amide protons were calculated using the overall correlation time (see below) and internuclear distances derived from the X-ray coordinates of the HIV-1 protease/DMP323

(41) Goldman, M. *Quantum Description of High-Resolution NMR in Liquids*; Clarendon Press: Oxford, U.K., 1984; Chapter 9.3.
(42) Ottiger, M.; Delaglio, F.; Bax, A. *J. Magn. Reson.* **1998**, *131*, in press.
(43) Tjandra, N.; Wingfield, P.; Stahl, S.; Bax, A. *J. Biomol. NMR* **1996**, *8*, 273−284.
(44) Wang, Y. X.; Freedberg, D. I.; Wingfield, P. T.; Stahl, S. J.; Kaufman, J. D.; Kiso, Y.; Bhat, T. N.; Erickson, J. W.; Torchia, D. A. *J. Am. Chem. Soc.* **1996**, *118*, 12287−12290.
(45) Kay, L. E.; Nicholson, L. K.; Delaglio, F.; Bax, A.; Torchia, D. A. *J. Magn. Reson.* **1992**, *97*, 359−375.
(46) Delaglio, F.; Grzesiek, S.; Vuister, G. W.; Zhu, G.; Pfeifer, J.; Bax, A. *J. Biomol. NMR* **1995**, *6*, 277−293.
(47) Ross, A.; Czisch, M.; King, G. C. *J. Magn. Reson.* **1997**, *124*, 355−365.

complex[48] in the following way. Seven sources of relaxation were included in the calculation: (1) dipolar interaction between ^{1}H and its directly attached ^{15}N, (2) ^{1}H−^{1}H dipolar interaction between amide protons, (3) dipolar interaction between the amide ^{1}H and slowly exchanging hydroxyl protons (i.e., hydroxyl protons that are seen in the crystal structure and have assigned NOEs to amide protons), (4) ^{1}H−^{1}H dipolar interaction between the amide protons and protons in DMP323, (5) ^{1}H−^{1}H dipolar interaction between the amide protons and the residual (∼15%[44]) α- and β-protons in the perdeuterated sample (6) ^{1}H−^{2}H dipolar interaction between the amide and neighboring α- and β-deuterons (i.e., ∼85%), and (7) amide ^{1}H chemical shift anisotropy (CSA). Cross correlations between the ^{1}H−^{15}N dipolar interaction and ^{1}H CSA and between the ^{1}H-^{15}N and ^{1}H−^{1}H dipolar interactions were suppressed by applying a ^{15}N 180° pulse at the center of the spin-locking period.[45,49] Although cross correlations of ^{1}H−^{1}H dipolar and ^{1}H CSA interactions are not eliminated by our pulse sequences, the effect of these cross correlations should be quite small for several reasons. First, perdeuteration restricts dipolar cross correlations primarily to amide protons. Second, neither the ^{1}H−^{1}H dipolar interactions nor the ^{1}H CSA typically make a large contribution to the ^{1}H relaxation mechanism. Third, the *z*-principal axis of the largest ^{1}H−^{1}H dipolar interaction, typically between amide protons in a helix, does not generally align with *z*-principal axis of the ^{1}H CSA. Furthermore, in a helix, the ^{1}H CSA is particularly small, ca. 5 ppm.[50] Fourth, in the spin-locking experiments, relatively short relaxation delays were employed (to minimize sample heating by the RF field), and this minimizes the effect of cross correlation on the relaxation rate extracted from the data.[20] Finally, we note that the spin-diffusion mechanism has little effect on $R_{1\rho}$ measurements and is further diminished by deuteration.

Under the conditions used in our experiments, $J(\omega_1)$ nearly equals $J(0)$ where ω_1 is an angular frequency of the applied RF field.[51] The overall correlation time of the protease/DMP323 complex, τ_R, is 11.9 ns at 20 °C from ^{15}N relaxation experiments (data not shown). This implies that the slow tumbling limit condition, $(\omega_H\tau_R)^2 \gg 1$, is satisfied, where ω_H is the ^{1}H Larmor precession frequency. In this limit, the spectral density functions containing ω_H are less that 1% of $J(0)$ and can be safely neglected. Hence, only $J(0)$ and $J(\omega_N)$ were included in the calculation. S^2 values, the generalized order parameters,[40,52] for the amide protons at 20 °C are assumed to be the same as those for amide ^{15}N determined at 35 °C previously.[39] Given the values of S^2 and τ_R, the $(1-S^2)$ term[40,52] contributes ca. 1% or less to the spectral density function and is omitted. Thus, the amide proton relaxation rates for the various interactions have the following simple expressions:

For ^{1}H−I dipolar interaction, where I = ^{15}N or ^{2}H

$$R_{1\rho} = (4/20)(4/3)I(I+1)\gamma_H^2\gamma_I^2(h/2\pi\, r_{HI}^3)^2S^2 \times \{\tau_R + (3/4)\tau_R/(1+\omega_I^2\tau_R^2)\} \quad (1)$$

For ^{1}H−^{1}H dipolar interaction (unlike spins)

$$R_{1\rho} = (5/20)\gamma_H^4(h/2\pi r_{HH}^3)^2S^2\tau_R \quad (2)$$

For ^{1}H−^{1}H dipolar interaction (like spins)

$$R_{1\rho} = (9/20)\gamma_H^4(h/2\pi r_{HH}^3)^2S^2\tau_R \quad (2a)$$

For ^{1}H CSA

$$R_{1\rho} = (4/45)(\sigma_{||} - \sigma_\perp)^2(2\pi\omega_H)^2S^2\tau_R \quad (3)$$

Here, $I(I+1) = 3/4$ for ^{15}N and 2 for ^{2}H, γ is magnetogyric ratio, and r is the internuclear distance. In eq 3, $\sigma_{||} - \sigma_\perp$, the chemical shift anisotropy, is assumed to be 10 ppm.[50] In eqs 2 and 2a, the relaxation rate was multiplied by 0.9 to account for the dilution of the labile protons by the 10% ^2H_2O in the NMR sample.

Results and Discussion

^{1}H Transverse Relaxation of a Perdeuterated Protein. The protease homodimer contains 99 residues in each monomer. The residues in each monomer have identical chemical shifts, demonstrating that the average dimer conformation is symmetric. Typically, we refer to each pair of residues in the two monomers by the same residue number. All amides have been assigned[36,53] and relaxation rates of 86 amide protons in each monomer were obtained using $R_{1\rho,unlike}$, CPMG, and Hahn-echo pulse sequences. Examination of Figure 2A shows that the $R_{1\rho,unlike}$ values were the same as those of CPMG R_2 for nearly all residues in the protein. This result is in accord with our expectation that, if R_{ex} is negligible, the relaxation rates are those of unlike spins. For eight residues, 6, 26, 31, 51, 91, 93, 95, and 98, differences in relaxation rates measured by these experiments are observed. Specifically, for each of these residues, we find that CPMG R_2 < Hahn-echo R_2 as shown in Figure 2B. The observed decrease in relaxation rate as the effective time for free-precession decreases, i.e., $R_{1\rho,unlike}$ < CPMG R_2 < Hahn-echo R_2, indicates that the relaxation rates, R_2, of these protons contain an R_{ex} contribution. As we discuss later, the R_{ex} contribution is due to exchange of chemical shifts on the time scale of ca. 1 ms.

Further insight into the amide spin dynamics is obtained by comparing the relaxation rates measured by the $R_{1\rho,unlike}$ and $R_{1\rho}$ experiments (Figure 2C). The general result evident in the figure is that $R_{1\rho}$ is greater than $R_{1\rho,unlike}$. A closer examination of the data reveals the more interesting result that the differences between the $R_{1\rho,unlike}$ and $R_{1\rho}$ relaxation rates are most pronounced for residues having the largest relaxation rates. These residues are those having the largest ^{1}H−^{1}H dipolar interactions. As noted earlier, the protons relax as like spins in the $R_{1\rho}$ experiment and as unlike spins in the $R_{1\rho}$ experiment, and eqs 2 and 2a predict that the ratio of ^{1}H−^{1}H relaxation rates is 9/5. A plot of $R_{1\rho}$ vs $R_{1\rho,unlike}$, Figure 2D shows slope of 1.7, in a good agreement with the value of 1.8 expected theoretically. Later, we show that those residues with the largest relaxation rates have the largest predicted ^{1}H−^{1}H dipolar interactions based upon the coordinates of the protease/DMP323 crystal structure.

Because the ^{1}H−^{1}H dipolar interaction makes a smaller contribution to $R_{1\rho,unlike}$ than to $R_{1\rho}$, the former experiment is more sensitive to R_{ex} contributions to relaxation than the latter. However, the development of ROESY cross-peaks in the $R_{1\rho,unlike}$ experiment, in principle, results in nonexponential

(48) Lam, P. Y.; Jadhav, P. K.; Eyermann, C. J.; Hodge, C. N.; Ru, Y.; Bacheler, L. T.; Meek, J. L.; Otto, M. J.; Rayner, M. M.; Wong, Y. N.; Cheng, C. H.; Weber, P. C.; Jackson, D. A.; Sharpe, T. R.; Erickson-Viitanen, S. *Science* **1994**, *263*, 380−384.
(49) Palmer, A. G.; Skelton, N. J.; Chazin, W. J.; Wright, P. E.; Rance, M. *Mol. Phys.* **1992**, *75*, 699−711.
(50) Tjandra, N.; Bax, A. *J. Am. Chem. Soc.* **1997**, *119*, 8076−8082.
(51) Jones, G. P. *Phys. Rev.* **1966**, *148*, 332−335.
(52) Lipari, G.; Szabo, A. *J. Am. Chem. Soc.* **1982**, *104*, 4559−4570.
(53) Yamazaki, T.; Nicholson, L. K.; Torchia, D. A.; Stahl, S. J.; Kaufman, J. D.; Wingfield, P. T.; Domaille, P. J.; Campbell-Burk, S. *Eur. J. Biochem.* **1994**, *219*, 707−712.

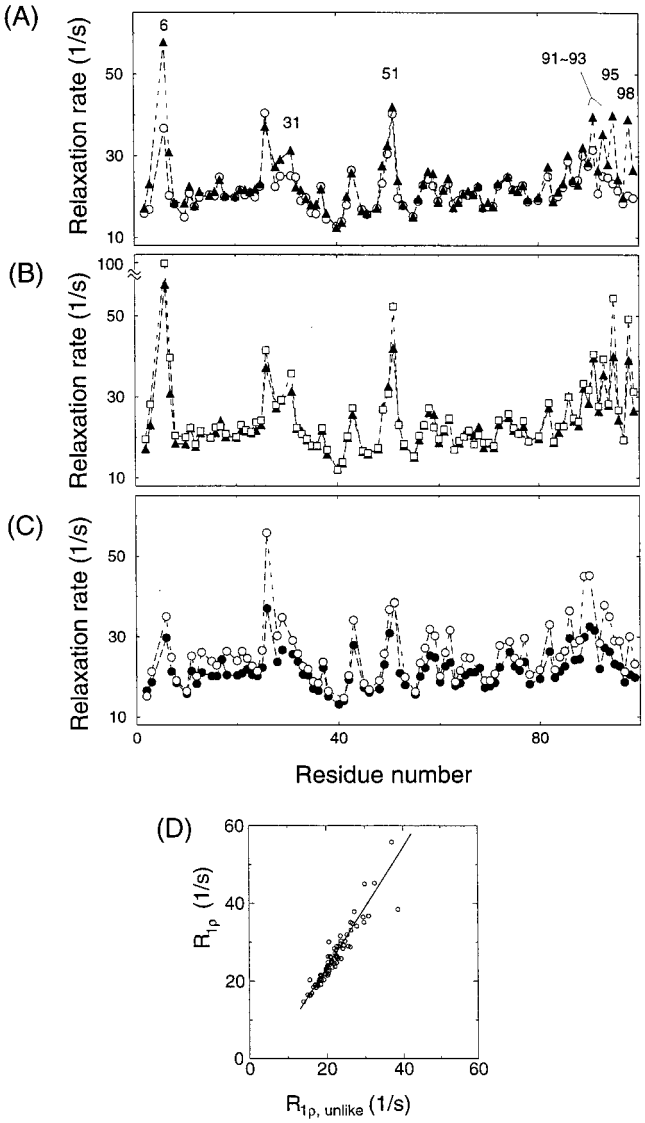

Figure 2. Comparison of various types of amide proton transverse relaxation rates, measured at 500 MHz and 20 °C, plotted as a function of HIV-1 protease residue number: (A) CPMG R_2 (▲), and $R_{1\rho,\text{unlike}}$ (○). (B) Hahn-echo R_2 (□) and CPMG R_2 (▲). In the CPMG pulse train $(-\tau_{CPMG}-180°-\tau_{CPMG}-)_n$, τ_{CPMG} was set to 3 ms. Note that residue 6 has an exceptionally large Hahn-echo R_2 value and an error of ca. 20%. (C) $R_{1\rho,\text{unlike}}$ (●) and $R_{1\rho}$ (○). (D) Plot of $R_{1\rho}$ versus $R_{1\rho,\text{unlike}}$ showing a slope, 1.7, close to that expected from theory, 1.8.

magnetization decay. This is a minor problem in the perdeuterated sample because ^{1}H spin relaxation is not dominated by the proton dipolar interaction and because the relaxation delays used in the experiments were short, <36 ms. Numerical simulations show that fitting the relaxation data with a single-exponential function introduces an error of less than 5% in the determination of the relaxation rate. Consistent with this error estimate, there was no systematic difference between $R_{1\rho,\text{unlike}}$ and R_2 determined by the Hahn-echo experiment (Figure 2A). ROESY cross-peaks do not interfere with the detection of an R_{ex} contribution because they do not depend on the strength of the RF field when the RF field is large compared to the off-resonance field.

It is noteworthy that ROE cross-peaks were also observed in CPMG spectra, but cross-peaks were not observed for protons whose chemical-shift differences were more than 1 ppm (data not shown). Generally, ROE cross-peaks develop when a pair of dipolar coupled protons have chemical shifts that differ by

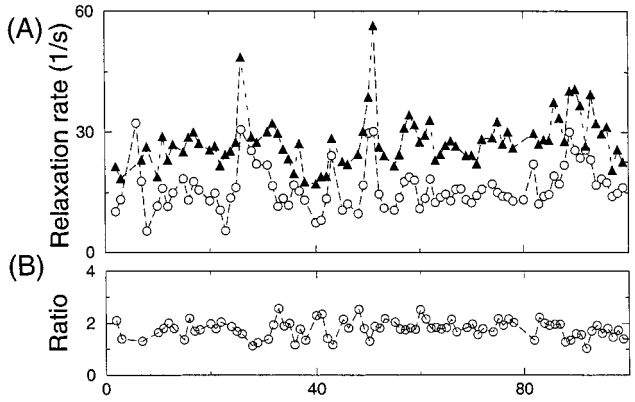

Figure 3. Comparison of $R_{1\rho,\text{unlike}}$ values of slow (upfield) and fast (downfield) relaxing components of the proton $^1J_{HN}$ doublets. (A) Slow (○) and fast (▲) components measured at 500 MHz and 20 °C, plotted as a function of residue number. (B) Ratio of the relaxation rates of fast and slow components.

an amount, $\delta\omega$, that is less than or equal to their cross relaxation rate, μ (i.e., the protons are effectively like spins).[41] Application of a CPMG sequence with $\tau_{CPMG} = 3$ ms partially aligns transverse magnetization of protons that have values of $\delta\omega$ up to ca. 200 Hz, permitting ROE cross-peaks to develop for such protons if they are dipolar coupled. Furthermore amide proton−amide nitrogen $^1J_{NH}$ coupling, ca. 95 Hz, attenuates dispersion of chemical shifts for those doublet components for which evolution of J and chemical shift partially cancel.

A further reduction of non-R_{ex} contributions to relaxation was achieved using the pulse scheme shown in Figure 1C, which utilizes cross correlation of ^{1}H−^{15}N dipolar and ^{1}H CSA interactions to attenuate the relaxation due to these mechanisms. The two signal components that arise from $^1J_{NH}$ coupling relax at different rates (Figure 3A); the relaxation rate of the upfield component is reduced due to partial cancellation of dipolar and CSA local fields while the relaxation rate of the downfield component is enhanced by the addition of dipolar and CSA local fields. Figure 3B shows that the ratio of the relaxation rates of the doublet components is ∼1.8 at 500 MHz, close to the value, ∼1.6, calculated as described in the next section. This ratio is much smaller than that of an isolated ^{15}N spin, ∼7,[45] because ^{1}H−^{1}H dipolar interactions contribute measurably to the relaxation of both ^{1}H doublets. In addition, the ratio of the CSA to dipolar interaction is smaller for the proton at 500 MHz than for ^{15}N, particularly for protons that are not in β-sheets.[50] Even so, the upfield components have the smallest $R_{1\rho,\text{unlike}}$ values that we have measured, less than 15 s^{-1} for many residues. The drawback of the $R_{1\rho,\text{unlike}}$ IPAP experiment is the significant reduction in signal-to-noise ratio associated with the detection of only one doublet component. However, when signal-to-noise allows, the $R_{1\rho,\text{unlike}}$ IPAP experiment is the most sensitive means to detect the presence of R_{ex} contributions to ^{1}H relaxation.

Comparison of Measured with Calculated $R_{1\rho,\text{unlike}}$ Relaxation Rates. Theoretical values of the dipolar contributions to $R_{1\rho,\text{unlike}}$ were calculated using eqs 1 and 2 and internuclear distances derived from the coordinates of the crystal structure of the HIV-1 protease/DMP323 complex, while the CSA contributions were calculated using eq 3. For the sake of clarity, the contributions to $R_{1\rho,\text{unlike}}$ were separated into the four components as shown in Figure 4A. We discuss the calculation of these four components in detail below.

(I) The directly bonded ^{1}H−^{15}N dipolar and ^{1}H CSA interactions (contributions 1 and 7, Materials and Methods) contribute relaxation rates of 10 and 0.4 s^{-1}, respectively, when

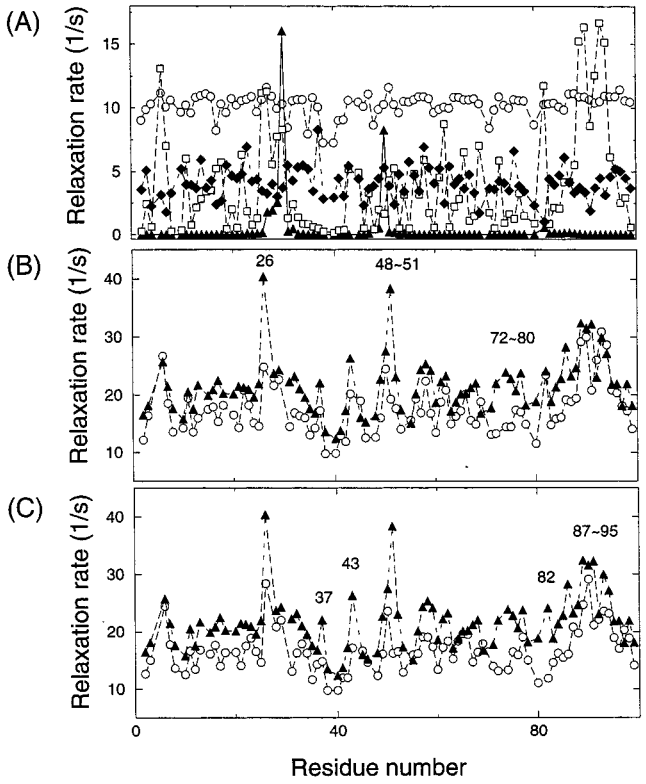

Figure 4. (A) Individual contributions to the calculated $R_{1\rho,\text{unlike}}$ values using internuclear distances derived from the X-ray coordinates of the HIV-1 protease/DMP323 complex and (B, C) comparison of the calculated $R_{1\rho,\text{unlike}}$ values with those measured at 20 °C. Panel A shows the following contributions to the amide proton relaxation rate of monomer 1 of the protease: dipolar interaction with the directly bonded amide nitrogen and ^{1}H CSA(○); dipolar interactions with amide protons or hydroxyl protons (□); dipolar interactions with protons in DMP323 (▲); dipolar interactions with α- or β-protons or deuterons (◆). The calculated value is shown only when the corresponding measured $R_{1\rho,\text{unlike}}$ is available. See text for details of the calculations. Measured relaxation rates (▲) are compared with the rates (○) calculated using internuclear distances derived from the X-ray coordinates of monomer 1 in panel B and monomer 2 in panel C.

S^2 is 0.85. Except for internal motion, these contributions would be site independent because the ^{15}N−^{1}H distance and the amide ^{1}H CSA are assumed to be the same for all amides. An approximate value for the proton CSA of 10 ppm was used in eq 3 for all residues. The projection of the ^{1}H CSA onto the NH bond axis was found to vary from 6 to 12 ppm in solution,[50] while amide proton (deuteron) CSA values of 13−14 ppm have been measured in the solid state.[54,55] While we do not know the precise value of the proton CSA in solution, our use of 10 ppm results in a contribution to the relaxation rate of ca. 0.4 s^{-1} and causes an error of less than 3% in the total calculated relaxation rate provided that the true ^{1}H CSA is in the range 5−14 ppm. Inter-residue ^{1}H−^{15}N dipolar interactions are less than 1% of the directly bonded ^{1}H−^{15}N dipolar interactions and are therefore not included in the calculations.

(II) The relaxation rates due to ^{1}H−^{1}H dipolar interactions between amide protons and between amide protons and slowly exchanging hydroxyl protons (contributions 2 and 3 described in the Materials and Methods). These rates range from 0 to 15 s^{-1} because the distances between each amide proton and its closest neighboring protons vary from ca. 2.2 to over 4 Å. For example the amide protons in the α-helix, spanning residues 87−94, have large ^{1}H−^{1}H dipolar interactions. These are clearly evident in Figure 4A and are a consequence of the short sequential amide proton distances in an α-helix.[56] The amide ^{1}H−^{2}H dipolar interactions are ca. 0.6% of that of amide ^{1}H−^{1}H dipolar interactions and are therefore not included in the calculations.

(III and IV) The contribution of ^{1}H−^{1}H and ^{1}H−^{2}H dipolar interactions from α- or β-protons/deuterons (contributions 5 and 6 in the Materials and Methods) is about 3 s^{-1}, of which the contributions from ^{1}H−^{2}H dipolar interactions are ca. 0.6 s^{-1}. These contributions are calculated assuming that the α- and β-positions are 15%/85% protonated/deuterated. Finally, the contributions from protons in DMP323 to amide proton relaxation are negligible except for residues 29 and 50.

Overall, the calculations show that the calculated relaxation rates range from 11 to 31 s^{-1} in the deuterated sample. These rates are 2−3-fold smaller than those calculated for the protonated protein.

Although each of the two monomer components of the protease has the same chemical shifts and average structure in solution, the two monomer conformations are slightly different in the crystal. Hence measured $R_{1\rho}$ values were compared with $R_{1\rho,\text{unlike}}$ values calculated using the crystal structure of monomer 1 (Figure 4B) and monomer 2 (Figure 4C). Overall the calculated $R_{1\rho,\text{unlike}}$ values are somewhat smaller than those observed, for reasons that are discussed later. Otherwise there is a good agreement between the calculated and measured $R_{1\rho,\text{unlike}}$ values for most residues in both monomers, demonstrating that the relaxation mechanisms employed in the calculations account for the relaxation that is observed. Residues 26, 37, 43, 48−51, 72−80, 82, and 87−95 (Figure 4B and/or 4C) are exceptions to this statement. It is interesting that not only do the calculated and measured values of $R_{1\rho,\text{unlike}}$ differ for these residues but the calculated values themselves differ for residues at equivalent sites in the two monomers (e.g., compare results for residues 26 and 82 in Figures 4B with results in Figure 4C), due to the aforementioned small difference in the two monomers in the crystal structure.

The observed differences between the calculated and measured $R_{1\rho,\text{unlike}}$ are not surprising when one considers the structural and dynamic characteristics of the residues for which the differences are observed. Residues 37 and 43 are located in or adjacent to a large flexible loop at the tips of the protease flaps, while residues 48−51 are located at the flexible β-turn at the flap elbows.[39] Although residues 26 and 82 are not flexible, their amides are close to the hydroxyl protons of Thr26 and Thr80, respectively, in the crystal, and amide NH−Thr OH NOEs are observed in the 3D ^{15}N separated NOESY spectrum. Like other hydrogen atoms, hydroxyl hydrogens of threonine are not seen in electron density maps of proteins, but unlike backbone amide and most aliphatic hydrogen atoms, these hydrogens cannot be precisely located upon the basis of covalent geometry because rotation about the C_γ−OH bond is not restrained. Hence the positions of Thr hydroxyl hydrogens are determined by steric and hydrogen-bonding criteria and are therefore not highly accurate. Because the relaxation rate is proportional to r^{-6}, even a small error in a hydroxyl proton position translates into a larger error in the calculated relaxation rate.

Another source of discrepancy between the calculated and measured $R_{1\rho,\text{unlike}}$ values arises from the fact that dipolar

(54) Gerald, R. N.; Bernhard, T.; Haeberlen, U.; Rendell, J.; Opella, S. *J. Am. Chem. Soc.* **1993**, *115*, 777−782.
(55) Ramamoorthy, A.; Wu, C. H.; Opella, S. J. *J. Am. Chem. Soc.* **1997**, *119*, 10479−10486.
(56) Wuthrich, K. *NMR of Proteins and Nucleic Acids*; John Wiley & Sons: New York, 1986.

interactions involving side-chain protons beyond the β-carbon were not included in the calculation because these positions are often flexible and not precisely defined in solution. Residues 72−78 are sandwiched by β-strands and fully buried in the protein interior. The amide protons of these residues are close to methyl groups of Ile62, Ile72, Thr74, Val75, Leu76, and Val78. Hence it is not surprising that the measured $R_{1\rho,\text{unlike}}$ values for residues from 72 to 78 are higher than the calculated ones. In general, the measured values of $R_{1\rho,\text{unlike}}$ are slightly larger than those calculated for a similar reason. If desired, the small contribution of dipolar interactions involving the residual side chain protons to the relaxation rate could be further reduced by increasing the level of deuteration. Finally, we note that neglect of anisotropic overall reorientation[50] introduces a root mean square (rms) error of 4−5% in the calculated values of the amide relaxation rates; however, this will not affect the determination of R_{ex}. In our analysis, R_{ex} is determined from the B_1 dependence of the relaxation rate or from relaxation rate differences and does not depend on assumptions about the overall reorientation of the molecule.

Dynamics of HIV-1 Protease Bound to DMP323 Derived from ^{1}H Transverse Relaxation. As noted earlier, the R_2 values of residues 6, 26, 31, 51, 91, 93, 95, and 98 are larger than the values of $R_{1\rho,\text{unlike}}$ measured for the same residues at 20 °C (Figure 2A). We interpret this observation as evidence that these residues experience an R_{ex} contribution to their relaxation rates. We model this motion as an exchange between two sites, A and B, having an exchange lifetime τ_{ex}, a chemical shift difference $\delta\omega$, and fractional populations p_{A} and p_{B}, where $p_{\text{A}} + p_{\text{B}} = 1$. The fast exchange limit, $(\delta\omega\ \tau_{\text{ex}})^2 \ll 1$, is satisfied because only a single (exchange averaged) chemical shift is observed for each amide ^{1}H and ^{15}N spin in the protein. In this limit, the exchange of chemical shifts contributions to the Hahn-echo, CPMG, and $R_{1\rho,\text{unlike}}$ relaxation rates are given by[57]

$$\text{Hahn-echo:}\quad R_{\text{ex}} \cong (\delta\omega)^2 p_{\text{A}} p_{\text{B}} \tau_{\text{ex}} \tag{4}$$

$$\text{CPMG:}\quad R_{\text{ex}} = (\delta\omega)^2 p_{\text{A}} p_{\text{B}} \tau_{\text{ex}} \times \{1 - \tau_{\text{ex}}/\tau_{\text{CPMG}} \tanh(\tau_{\text{CPMG}}/\tau_{\text{ex}})\} \tag{5}$$

$$R_{1\rho,\text{unlike}}\text{:}\quad R_{\text{ex}} = (\delta\omega)^2 p_{\text{A}} p_{\text{B}} \tau_{\text{ex}}/(1 + \omega_1{}^2 \tau_{\text{ex}}{}^2) \tag{6}$$

Note that eq 4 is a good approximation when $\tau_{\text{ex}} \ll T_{\text{HE}}$, where T_{HE} is the initial Hahn-echo relaxation delay, 6 ms in our experiments. When the intrinsic relaxation rates of the two sites are approximately equal, eq 5 is valid except for the case of slow exchange and large pulse separation.[58,59] Note that when $\omega_1{}^2\tau_{\text{ex}}{}^2 > 5$ (i.e., when $\tau_{\text{ex}} > 2 \times 10^{-4}$ s in our experiments) the exchange contribution to R_2 is over five times greater than it is to $R_{1\rho,\text{unlike}}$. This explains why $R_2 > R_{1\rho,\text{unlike}}$ for the residues affected by exchange and why the measured $R_{1\rho,\text{unlike}}$ values are independent of the strength of the spin-lock field at 20 °C. Our observation that $R_{1\rho,\text{unlike}} <$ CPMG($\tau_{\text{CPMG}} = 3$ ms) $R_2 <$ Hahn-echo R_2, together with the above equations for R_{ex}, indicates that τ_{ex} is ca. 1 ms at 20 °C for the residues noted above.

When the measured rates are compared at 35 °C (Figure 5A) differences between R_2 and $R_{1\rho,\text{unlike}}$ become smaller than the rate differences obtained at 20 °C. This observation is reasonable because the value of τ_{ex} is expected to decrease with an increase in temperature, decreasing the R_{ex} contribution to R_2. Differences between R_2 and $R_{1\rho,\text{unlike}}$ are however still significant at 35 °C for two residues, Thr4 and Trp6. It is noteworthy that B_1-field dependence of $R_{1\rho,\text{unlike}}$ is observed for Thr4 at 35 °C (Figure 5B), whereas at 20 °C, the effect of exchange of chemical shifts is so large that we do not observe Thr4 signals in either the Hahn-echo or CPMG experiments and only weak, broad signals in the $R_{1\rho,\text{unlike}}$ experiments (data not shown). These observations are entirely consistent with the presence of a strong ^{1}H exchange of chemical shifts effect for Thr4. At 35 °C, the exchange of chemical shifts effect is reduced and the line width of Thr4 is sufficiently narrow that we have sufficient signal-to-noise to measure its relaxation rates. At the same time, the exchange of chemical shifts effect at this temperature is sufficiently large that the B_1-field dependence is observable.

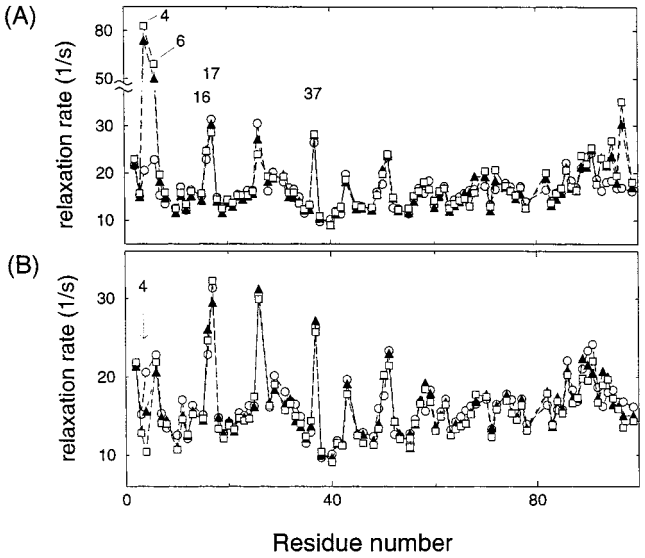

Figure 5. Comparison of (A) relaxation rates measured at 500 MHz and 35 °C using CPMG (▲), Hahn-echo (□) sequences, and $R_{1\rho,\text{unlike}}$ (○) and (B) $R_{1\rho,\text{unlike}}$ values measured at various spin-lock field strengths: (A) Hahn-echo (□), CPMG, $\tau_{\text{CPMG}} = 3$ ms (▲), and $R_{1\rho,\text{unlike}}$, 2-kHz spin-lock field (○); (B) $R_{1\rho,\text{unlike}}$ 2 kHz (○), 8 kHz (▲), and 12 (□) kHz spin-lock fields. Error for residues 4 and 6 was 6% for Hahn-echo and 8% for CPMG R_2. Note that $R_{1\rho,\text{unlike}}$ values for residues 16, 17, and 37 are larger than those measured at 20 °C (Figure 2A) because of rapid amide proton exchange with solvent water at 35 °C.[61]

Thr4, Leu5, and Trp6 are located in a solvent-exposed loop that contains the prime autolysis site of the protease. In previous studies, slow motion of this loop was inferred from the absence of the Leu5 cross-peak from the HSQC spectrum of the protease/DMP323 complex, which was presumed broadened beyond detectable limits. (We have not observed the Leu5 signals in the spectra of the protease bound to any one of four different inhibitors.) However, the model free analysis of the R_1, R_2, and NOE of ^{15}N relaxation data did not itself provide evidence of exchange broadening for either residues Thr4 or Trp6. Hence, the results obtained herein are the first direct evidence for slow motion at this site in the protein which may have functional significance due to its sensitivity to autolysis.

^{15}N Transverse Relaxation of Perdeuterated HIV-1 Protease. As we discussed above, comparison of CPMG R_2 and $R_{1\rho}$ is a powerful method to detect exchange of chemical shifts on the millisecond time scale. However, one cannot accurately measure the ^{15}N transverse relaxation using $\tau_{\text{CPMG}} > 2$ ms in a protonated protein because ^{1}H spin-flips enhance the relaxation rate of the $H_zN_{x,y}$ component created during the τ_{CPMG} period.[45]

(57) Mandel, A. M.; Akke, M.; Palmer, A. G. R. *Biochemistry* **1996**, *35*, 16009−16023.
(58) Allerhand, A.; Gutowsky, H. S. *J. Chem. Phys.* **1964**, *41*, 2115−2126.
(59) Allerhand, A.; Gutowsky, H. S. *J. Chem. Phys.* **1965**, *42*, 1587−1598.

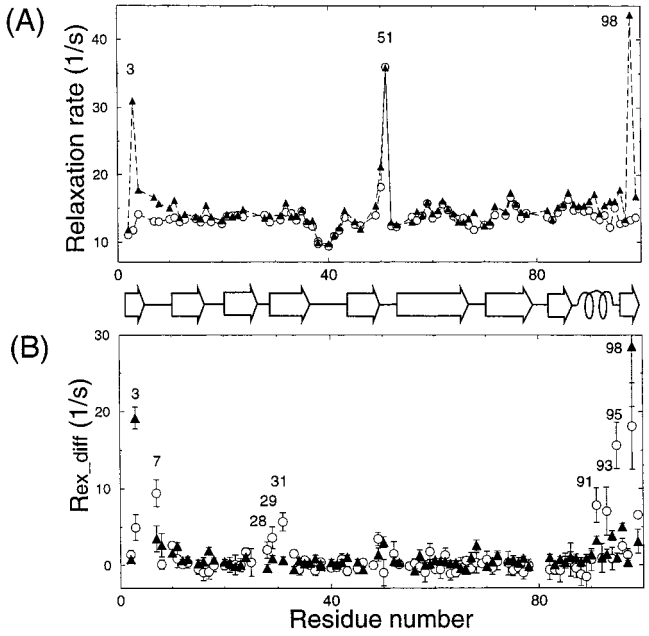

Figure 6. Comparison of (A) ^{15}N relaxation rates measured using CPMG R_2 (▲) and $R_{1\rho}$ (○). ^{15}N relaxation data were acquired at 500 MHz and 20 °C using spin-lock fields of 2 kHz and τ_{CPMG} of 3 ms. (B) Comparison of ^{1}H (○) and ^{15}N R_{ex_diff} (▲) defined in eq 7. $R_{1\rho,unlike}$ measured with a 2-kHz spin-lock field and R_2 measured with a τ_{CPMG} of 3 ms were used to calculate proton R_{ex_diff}, while the R_2 and $R_{1\rho}$ values shown in panel A were used to calculate ^{15}N R_{ex_diff}. Note that residue 7 has an error of 8% in ^{15}N $R_{1\rho}$ in panel A.

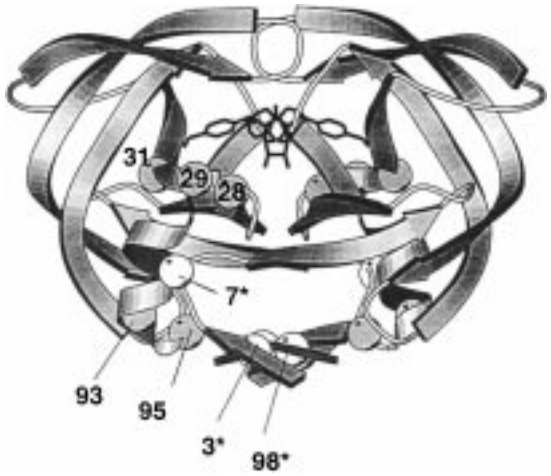

Figure 7. Protease amide sites having large values of $(\delta\omega_H/\delta\omega_N)^2$ (gray spheres) and medium values of $(\delta\omega_H/\delta\omega_N)^2$ values (white spheres). See the text for the classification of $(\delta\omega_H/\delta\omega_N)^2$ values. Residues in the second monomer have numbers labeled with a "*".

For example, in a typical protonated protein with the molecular size of 20 kDa, the H_zN_z relaxation rate, which is governed by NH proton spin-flip rate, is ca. 12 s^{-1} at 20 °C. Since the ^{15}N transverse relaxation rate is ca. 15 s^{-1}, the spin-flip effect causes an increase in the apparent ^{15}N relaxation rate of over 15% when τ_{CPMG} exceeds 3 ms (data not shown). Hence, the CPMG R_2 values acquired with large τ_{CPMG} duration cannot be readily compared with $R_{1\rho}$. However, as is shown in Figure 6A, in our perdeuterated protein, ^{15}N CPMG R_2 values were almost the same as ^{15}N $R_{1\rho}$ values, with an average CPMG R_2 only 3% higher than that of $R_{1\rho}$, except for a few residues, e.g., 3, 49, 50, 51, and 98, expected to undergo exchange of chemical shifts. This result indicates that ^{15}N CPMG R_2 values obtained with $\tau_{CPMG} = 3$ ms are available as a tool to examine slow internal motion in perdeuterated proteins. The H_zN_z relaxation rate of our sample is ca. 3 s^{-1} (data not shown). Because the ^{15}N R_1 is ca. 1.5 s^{-1}, this implies that the ^{1}H-selective R_1 is only ca. 1.5 s^{-1}. Numerical simulations using ^{1}H-selective $R_1 = 1.5$ s^{-1} and ^{15}N $R_2 = 15$ s^{-1} show that ^{1}H spin-flips have very small effects, ca. 2%, on ^{15}N R_2 values measured with τ_{CPMG} less than 3 ms.

Combined Use of ^{1}H and ^{15}N Relaxation Data To Detect Slow Internal Motion. We have investigated R_{ex} contributions in more detail, by determining the quantity

$$R_{ex\_diff} = \text{CPMG}\, R_2 - R_{1\rho,unlike} \tag{7}$$

Using eqs 5 and 6

$$R_{ex\_diff} = (\delta\omega)^2 p_A p_B \tau_{ex}\{(1 - \tau_{ex}/\tau_{CPMG}\tanh(\tau_{CPMG}/\tau_{ex})) - 1/(1 + \omega_1^2\tau_{ex}^2)\} \tag{8}$$

Values of ^{15}N R_{ex_diff} at 20 °C were derived from measurements of ^{15}N CPMG R_2 and $R_{1\rho,unlike}$ values in Figure 6A and were compared with values of ^{1}H R_{ex_diff} as shown in Figure 6B. It is found that residues having large ^{1}H R_{ex_diff} rates do not necessarily have large values of ^{15}N R_{ex_diff}. We suggest that this observation is due to the fact that R_{ex_diff} is proportional to the square of $\delta\omega$, which means that a 2−3-fold difference in $\delta\omega$ for the two spins results in a 4−9-fold difference in their R_{ex_diff} values. The general result (eq 9) applies when (1) the same spin-locking field strengths and CPMG delays are used to measure the relaxation rates of both amide ^{1}H and ^{15}N spins and (2) a common exchange process (i.e., having the same p_A, p_B, and τ_{ex} values) determines the relaxation of both amide spins.

$$^1\text{H}\, R_{ex\_diff}/^{15}\text{N}\, R_{ex\_diff} = (\delta\omega_H/\delta\omega_N)^2 \tag{9}$$

The accuracy of $(\delta\omega_H/\delta\omega_N)^2$ values determined using eq 9 is limited by uncertainties in the measured values of R_2 and $R_{1\rho}$, since R_{ex_diff} is equal to the difference of these rates. However, when the value of R_{ex_diff} is large for at least one spin, we are able to obtain estimated values of $(\delta\omega_H/\delta\omega_N)^2$ using eq 9. These estimates are classified somewhat arbitrarily as large $(\delta\omega_H/\delta\omega_N)^2 > 3$, small $(\delta\omega_H/\delta\omega_N)^2 < 0.3$, and medium $0.3 < (\delta\omega_H/\delta\omega_N)^2 < 3.0$.

Residues 28, 29, 31, 93, and 95 have large values of $(\delta\omega_H/\delta\omega_N)^2$, while residues 3, 7, and 98 have medium values of $(\delta\omega_H/\delta\omega_N)^2$. Residues 28 and 29 interact with DMP323, while residues 93 and 95 are in the single α-helix in the protease. On the other hand, residues 3 and 98 are located in the β-sheets at the intermonomer interface and residue 7 is in the loop adjacent to the β-strand including residue 3.

Because the factors that determine the chemical shifts of ^{1}H and ^{15}N spins are not understood in detail, we cannot interpret these interesting local differences in $(\delta\omega_H/\delta\omega_N)^2$ values in terms of specific local conformational changes in the protein. However, a few general comments can be made. Spins whose distances from an aromatic ring vary will have $\delta\omega$ values proportional to their magnetogyric ratios, resulting in large values $(\delta\omega_H/\delta\omega_N)^2$. The amides of residues 28 and 29 are close to the aromatic rings of DMP323, while the several amides of helical residues 91−95 are close to the side chain of Trp6. Alternatively, fluctuations of the helix itself may cause a change in the local magnetic field produced by the helix dipole.[60] This

(60) Williamson, M. P. *Biopolymers* **1990**, *29*, 1423−1431.

would result in large values of $(\delta\omega_H/\delta\omega_N)^2$ as is observed for these residues.

In a folded protein the dispersion of ^{1}H and ^{15}N shifts is about the same, when measured in hertz, suggesting that fluctuations in (φ,ψ) angles or in the local environment would result in roughly comparable values of $\delta\omega$ for ^{1}H and ^{15}N spins. On this basis we suggest that the medium values of $(\delta\omega_H/\delta\omega_N)^2$ for residues 3 and 98 could reflect either (a) a cooperative internal motion for these near-terminal, but hydrogen-bonded, residues or (b) the motion of the loop consisting of residues 4−6 which causes fluctuations in their chemical shifts as well as that of residue 7.

Although the interpretation of $(\delta\omega_H/\delta\omega_N)^2$ values given above is speculative, it seems reasonable to suppose that, as quantitative calculations of chemical shifts continue to improve, insights about the conformational states involved in slow fluctuations within proteins will be provided by measurements of $(\delta\omega_H/\delta\omega_N)^2$. We are not aware that either $\delta\omega_H$ or $\delta\omega_N$ can be obtained from relaxation measurements of a single nucleus. In addition, for the reasons noted herein, when conformation exchange occurs at a particular amide site, it is possible that the R_{ex} contribution to relaxation for either the ^{1}H or ^{15}N nucleus is too small to detect. Hence we suggest that the complementary use of ^{1}H and ^{15}N transverse relaxation rates provides useful information about slow motions in proteins that cannot be obtained from measurements on either nucleus alone.

Acknowledgment. We thank Frank Delaglio and Dan Garrett for data processing software, Ad Bax for helpful discussions, Tom Bull and Nico Tjandra for critical reading of the manuscript, and DuPont Merck Pharmaceutical Co. for DMP323. This work was supported by the intramural AIDS Targeted Anti-Viral Program of the Office of the Director of the National Institutes of Health.

JA981546C

(61) Wang, Y. X.; Freedberg, D. I.; Grzesiek, S.; Torchia, D. A.; Wingfield, P. T.; Kaufman, J. D.; Stahl, S. J.; Chang, C. H.; Hodge, C. N. *Biochemistry* **1996**, *35*, 12694−12704.